An empirical Scherrer equation for weakly swelling mixed-layer minerals, especially illite-smectite

Article *in* Clay Minerals · December 1999

DOI: 10.1180/000985599546479

CITATIONS
32

READS
142

3 authors, including:

Michel Jaboyedoff
University of Lausanne
602 PUBLICATIONS **7,697** CITATIONS

SEE PROFILE

Clay Minerals (1999) **34**, 601–617

An empirical Scherrer equation for weakly swelling mixed-layer minerals, especially illite-smectite

M. JABOYEDOFF*,**, B. KÜBLER** AND PH. THÉLIN*

*Institut de Minéralogie et Pétrographie Université de Lausanne, BFSH2, 1015 Lausannne, Switzerland, and
**Institut de Géologie, Université de Neuchâtel, Rue Emile-Argand, 11, 2007 Neuchâtel, Switzerland

(*Received 23 February 1998; revised 10 May 1999*)

ABSTRACT: The Scherrer equation links the measured width of an X-ray diffraction peak (Scherrer width, SW) to the number of stacked cells (N) in the direction normal to the diffracting planes. The formula is only valid for one d-value occurring in the coherently diffracting domain. This equation can be modified for weakly swelling mixed-layer minerals. This assumes that the peak broadening caused by the mixed-layering is proportional to the amount of swelling component (S) and that the effects of size and mixed-layering are additive.

If two SW can be measured on XRD patterns from samples treated in two different ways (such as air dried or glycolated), N and S can be determined. This equation is applicable to illite-smectite mixed-layer minerals with high illitic content. The results are most accurate for N>30. The use of Scherrer's equation is discussed.

Scherrer (1918) was the first to develop a method to determine the number of stacked cells by measuring the width of a diffraction peak, assumed to be Gaussian in shape. More precisely, the 'Scherrer width' (SW) measures the sharpness of the interference function which depends on the number of stacked cells in the coherent diffracting domains (CSD) and the d-spacing in the direction perpendicular to the reflecting planes (Klug & Alexander, 1974). Usually the Scherrer equation cannot provide a complete description of a mixed-layer mineral containing expandable interlayers, such as an illite-smectite (I-S), because more than one d-spacing is present and the associated structure factors for the interlayers are different.

Since the SW of mixed-layer minerals is not determined solely by the CSD size, the best way to verify estimates of the CSD size and of the amount of mixed layering is to perform XRD pattern simulation. To obtain a first estimate of the CSD size and the amount of mixed layering only a few simple methods are available. For example, methods such as the measurement of peak positions give only information on the amount of mixed layering. Furthermore, they are not applicable to mixed-layer minerals containing small numbers of swelling interlayers. More sophisticated methods, such as the Bertaut-Warren-Averbach method can be applied (Drits *et al.* 1998), but they give the CSD size only, and for more information other methods are needed (Eberl *et al.* 1998).

In this paper, we consider the case of a mixed-layer mineral containing a small number of swelling interlayers, for which XRD patterns of two different treated specimens (e.g. air-dried (AD) and ethylene-glycol treated (EG)) are available. The peak positions of the two different XRD patterns are not significantly shifted, but their SW can change. Assuming that the peak broadening is linearly dependent on the amount of swelling layers, this amount can be determined, as well as the CSD size, by measurements of the width at half maximum of the corresponding peak on the XRD patterns of the two treatments.

The goal of this paper is to establish a relationship between the Scherrer width (SW) and the CSD size and to formulate an empirical version of the Scherrer equation, which can be applied to a two-component mixed-layer mineral. Thus, for example, one XRD peak's SW measured on the AD pattern (SWAD) and on the EG (SWEG) patterns, leads to estimations of both the CSD size (N) and the amount of swelling interlayers (%S), here usually assumed to be a smectitic interlayer. This procedure then enables a simulation of the diffraction pattern to be performed, using a programme such as Newmod©, to check the validity of the assumptions. If the number of layers is too high for the simulation programme (it is limited to 100 in Newmod©) the empirical equation presented here gives an estimate of N and %S.

MEASUREMENT OF THE SW

In order to analyse the diffraction peak rigorously, the intensities must first be divided by the Lorentz-polarization factor and the square of the modulus of the structure factor and then the background removed (Drits *et al.*, 1998). The data used in this paper were not, however, treated in this manner because such procedures can give very different results if carried out in different ways. For example, the background as estimated by automatic procedures (e.g. Fourier transforms) often rises again within the peak area, which is not physically sensible.

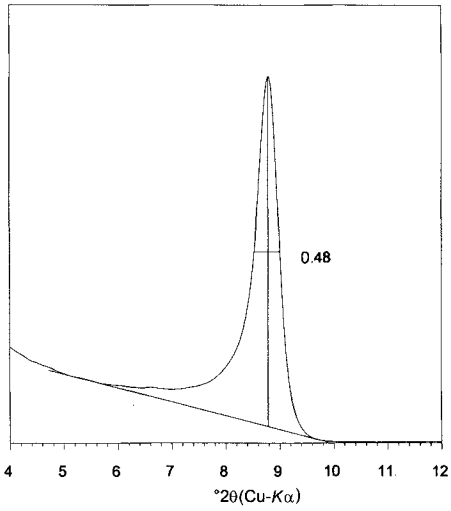

FIG. 1. Method to measure the SW using a Newmod© simulation (software: QUICKWIDTH).

There are many different ways to measure the SW (depending on the interpretation, SW does or does not include the instrumental broadening). Since the aim of the present work was to produce a simple method for estimating N and %S, we chose the simplest method (Fig. 1), consisting of tracing a linear background under the untreated raw data peak and measuring horizontally the width at half maximum above the background. This is equivalent to the traditional manual method of background measurement. It should be noted that few of the alternative methods give information on the SW in the sense originally adopted by Scherrer, because of the influence of the structure factor and the Lorentz-polarization factor on the diffraction pattern (e.g. Reynolds, 1968).

The approach proposed here is relevant for most background types, but the results presented are only strictly valid for our method of background measurement.

MEASUREMENT OF I-S 10 Å PEAK SW

This idea of SW measurement was extended to the illite or I-S mixed-layer minerals, i.e. materials giving a ~10 Å peak with high illite content (Kübler, 1964, 1967, 1984; Frey 1987), because the SW of illite usually decreases as the temperature of the setting in which the mineral is found increases. Considering only a two component mixed-layer, the IC ('illite crystallinity' index) method was chosen empirically because of its sensitivity to swelling interlayers in order to describe the lower step of the metamorphism. The method was first called 'illite crystallinity index' (IC), but the term illite Scherrer Width (ISW) is more appropriate, and the ISW is widely used because of its ease of measurement. The ISW includes the instrumental broadening effect. This measurement was found to be more reproducible than the previous index proposed by Weaver (1960) and Kübler (1967, 1968, 1990). It became successful also because peak position methods (Reynolds, 1980; Watanabe, 1988) cannot be applied to minerals with small amounts of mixed-layering since the peak's position does not migrate. According to Eberl & Velde (1989), the ISW can be related to CSD size and amount of mixed-layering, especially on the first basal 10 Å reflection, for which effects of interstratification

and CSD size are emphasized. As a result, in progressive low-grade metamorphism the decrease in IC values is essentially produced by the CSD increase and the decrease in number of swelling layers. Unfortunately the Eberl & Velde (1989) method uses ISW plus the IR ratio of Środoń & Eberl (1984), in which the 003 peak is taken into account. This can be a problem because the 003 peak is sometimes overlapped by a quartz peak (Moore & Reynolds, 1997).

The modern approaches involve decomposition of the 10 Å diffraction peak in different ways (Lanson & Velde, 1992; Lanson & Champion, 1991; Pevear & Schuette, 1993; Stern *et al.*, 1991; Wang *et al.*, 1995), but the ISW of the decomposition peaks must be coherent between AD and EG preparations, i.e. the number of XRD peaks must be in agreement with the number of 'phases' in both decompositions. Furthermore, the CSD size and their %S attached to each 'phase' must be equal for each preparation decomposition. Software such as NEWMOD© (Reynolds, 1985; Reynolds & Reynolds, 1996) and DECOMPXR (Lanson, 1990; Lanson & Velde, 1992) are very useful, but interpretation of diffraction patterns by simulation is often time-consuming.

Many authors proposed use of the 5 Å XRD peak of AD preparation to avoid the problems of the swelling interlayer (Eberl & Blum, 1993; Nieto & Sanchez-Navas, 1994; Warr, 1996). In this particular case, the estimated CSD size is correct using Scherrer's equation (Nieto & Sanchez-Navas, 1994; Arkai *et al.*, 1996). However for a sophisticated study, e.g. one using the Bertaut-Warren-Averbach method, the peak shape of the I-S interstratification is not perfectly identical to that produced by N equivalent layers of identical d-spacing. The correct way to apply such a method was described by Drits *et al.* (1998) and Eberl *et al.* (1998). Application of this method gives good results but expandable interlayers are missed; this is of some importance as the %S is one of the most sensitive parameters used to characterize diagenesis (see Moore & Reynolds, 1997, for general review).

Although measurement of the ISW is a rather old method, it is a very useful quick method to obtain information on regional low-grade metamorphism (Roberts & Merriman, 1985; Frey, 1988; Goy-Eggenberger & Kübler, 1990; Merriman *et al.*, 1990; Krumm, 1992; Wang *et al.*, 1995; Sassi *et al.* 1995; Jaboyedoff & Thélin, 1996; Arkai *et al.*, 1996; Arkai *et al.* 1997).

SCHERRER EQUATION

According to Méring (1949), Kodama *et al.* (1971), Reynolds (1980, 1989) and Eberl & Velde (1989), the SW depends mainly on: (1) the distribution of the CSD sizes (the 'size' is equal to the number of layers in each domain); (2) the presence of expandable or other kinds of interlayer (this can be a function of the particle size); (3) asymmetry due to the structure factor and the Lorentz polarization factor; (4) disorder (small variations of the d-spacing); and (5) instrumental effects, excluding the Lorentz-polarization factor. For example, in Newmod© simulation, neither the effect of the flat specimen, nor axial divergence broadening, nor receiving slit and instrumental background effects are taken into account.

The fifth effect may be removed either by an unfolding method (Stokes, 1948; Ergun, 1968) or by simpler methods. We define b as the maximum breadth or SW of the instrumental effect, B the SW measured on the unrefined profile and $\beta_{\Delta 2\theta}$ the estimated SW of the pure profile. In the case of a Lorentzian shape for all peaks, $\beta_{\Delta 2\theta}$ is then given by B-b, whereas for Gaussian peaks the result is $\beta_{\Delta 2\theta} = \sqrt{(B^2_{\Delta 2\theta} - b^2)}$. An intermediate solution is the geometric mean of the two previous solutions (Balasingh *et al.* 1991), i.e.

$$\beta_{\Delta 2\theta} = \sqrt{(B - b) \times \sqrt{B^2_{\Delta 2\theta} - b^2}} \qquad (1)$$

This method seems valid as it gives intermediate values between Lorentzian and Gaussian assumptions. Another solution, a little bit more time-consuming, is to construct a conversion table between the observed SW (B) and $\beta_{\Delta 2\theta}$, the SW of the pure profile. This table may be obtained by the convolution of the peak of a well crystallized mica powder, taken to be the instrumental profile, with a calculated pure profile assumed to be represented by a symmetrical Pearson-VII peak, with a power of 2 (Jaboyedoff, 1999). We used this solution in one of the following examples.

The Scherrer equation

$$\beta_{\Delta 2\theta(\mathrm{rad})} = \frac{\mathrm{K} \times \lambda}{L_{hkl} \times \cos\theta_0} \qquad (2)$$

can be then applied if it is assumed that only the first of the effects (1) to (3) listed above is significant, that the fourth one is not disturbing the profile, and that the fifth one is removed (Klug

& Alexander, 1974). $\beta_{\Delta 2\theta}$ is the full width at half maximum in radian units, λ the wave length, θ_0 the diffraction angle and K the Scherrer constant (Langford & Wilson, 1978) discussed in Drits *et al.* (1997). The value of K depends on the shape and on the distribution of the CSD. The mean thickness, L_{hkl}, of the CSD, given by $L_{hkl} = Nd$, N being the number of units of thickness d in the direction perpendicular to the plane *hkl*. For a population of CSD it is better to regard L_{hkl} as a measure of the square root of the mean-square values (i.e. an rms value) for small CSD, because the maximum of the interference function is proportional to N^2 (Figs. 2 and 3, curves 4 and 5). Note, however, that when N>20, the rms becomes close to standard arithmetic mean.

In this paper we use only the 00*l* lines for plate-like domains with a distribution for N possessing equal probabilities in a given range and zero outside. For small CSD, the rms can be used if necessary. The demonstration of the Scherrer equation given by Klug & Alexander (1974) is based only on the evaluation of the breadth of the interference function, which leads to a value of K = 0.89. The true width of the interference function and that derived from the Scherrer equation (Fig. 3, curves 1 and 2) are very similar. For a given θ_0 and λ equation (2) can be simplified to:

$$\beta_{\Delta 2\theta(\mathrm{deg})} = \frac{D}{N} \qquad (3)$$

in which N is the number of cells or sub-cells perpendicular to the diffraction planes, D is a constant deduced from the equation and $\beta_{\Delta 2\theta}$ is given in degrees. For example, for the 10 Å peak and λ = 1.5418 Å (Cu-$K\alpha$), D = 7.9.

The Scherrer equation cannot be applied directly to mixed-layer clay minerals when the expandable layers are swollen (Drits *et al.*, 1997), because it is only applicable when there is a single d-spacing. In the case of a population of a single d-spacing with lattice distortions, the size effect and lattice distortions can be separated by various methods, such as Fourier analysis or integral breadth method, etc. (see Warren & Averbach, 1950; Wilson, 1962; Kodama *et al.*, 1971; Klug & Alexander, 1974; Langford & Wilson, 1978; Drits & Tchoubar, 1990; Arkai *et al.*, 1996; Eberl *et al.*, 1997; Drits *et al.* 1998; Eberl *et al.*, 1998 and for a general review Delhez *et al.*, 1982).

The Scherrer equation (2 or 3) indicates a linear relationship between the SW of the interference

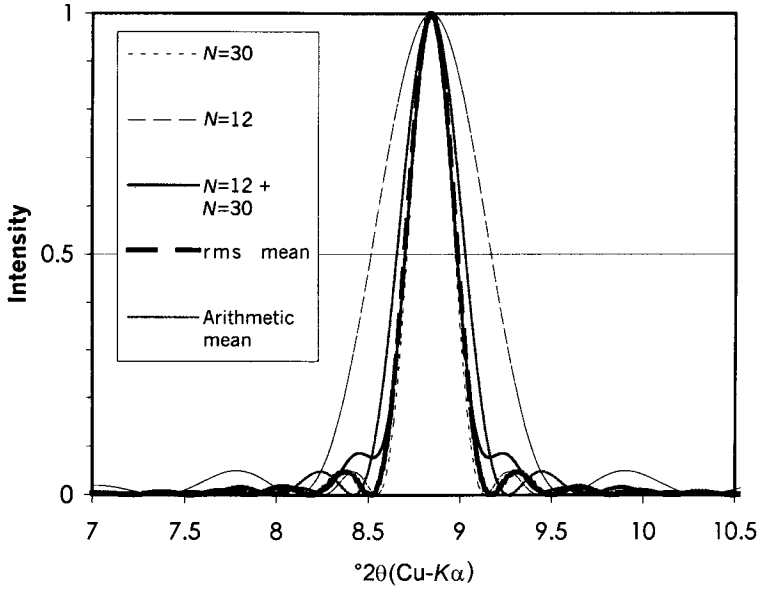

FIG. 2. Different interference functions from different methods (rms) of calculating the mean number of layers in coherent domains. Note that the square root of the mean-squares gives a better representation than the arithmetic mean for small values of N.

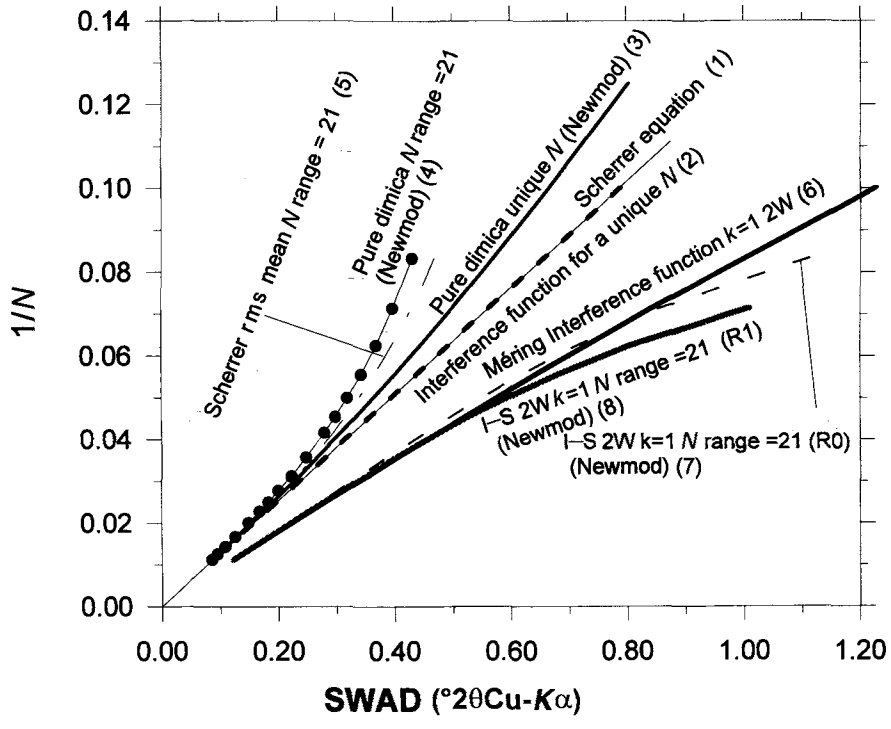

FIG. 3. Relationship between SWAD and the inverse of the mean of the number of layers N. The Scherrer equation is equivalent to the true SW of the interference function for a unique N (1 and 2). The single N illite SW (3) is slightly sharper than the Scherrer equation. Newmod© simulations have been performed on range of $N \pm 10$ with equal weights (4). These simulations display behaviour very similar to that obtained from the Scherrer equation with the rms mean (5). The SW of the Méring interference function (6) is consistent with a linear behaviour for $k = 1$ used to define %S, as a normal interference function. It is very similar to results obtained by Newmod© simulations with $k = 1$, equal probability N over a range of 21 centred on the mean value ($N \pm 10$) and Reichweite R0 (7), R1 (8) (two water layers). See the Results section for the Newmod© parameters (Dimica = dioctahedral mica).

function and the inverse of the number of layers N. When considering the third and the fifth contributions to the SW, it should be noted that removal of the instrumental broadening effect and application of a background correction are not sufficient to suppress the structure factor effect (the structure factor of mixed-layer minerals is complex) or the Lorentz polarization factor (Moore & Reynolds, 1997 chap. 3). These factors are very important when the number of layers is small (Reynolds, 1968). However, when the peak is narrow, the contribution from the structure factor and Lorentz-polarization factor does not vary too much and can be ignored. A linear relationship exists partially also, e.g. in the classical measurement of the SW of the 001 of pure dioctahedral mica and the inverse of N for high N Newmod© simulations without removal of the third contribution, ignoring the fourth and eliminating the fifth (Fig. 3, curves 3 and 4).

EMPIRICAL SCHERRER EQUATION FOR WEAKLY SWELLING MIXED-LAYER MINERALS

When the material is a mixed-layer mineral containing swollen interlayers, it is difficult to consider the effects of disorder (i.e. small variations in the d-spacing, point 4 in the list of parameters) with a simple approach. Therefore, in the following sections, we deal only with the first and second

effects assuming a two component mixed-layer mineral.

As a first approximation, the broadening due to the expandable interlayers is supposed to be proportional to their percentage, %S, for a Reichweite R0 (for definition of R, see Jadgozinski, 1949; Drits & Tchoubar, 1990; Moore & Reynolds, 1997). In this case a broadening term must be added to the Scherrer equation (which is the CSD contribution). To simplify the problem of those two terms, a relation between the number of layers and the number of expandable interlayers must be chosen. The SW is inversely proportional to the number of layers of the CSD, according to the Scherrer equation. Therefore, the simplest choice is to consider the amount of expandable interlayers as being inversely proportional to the number of layers by a factor k leading to:

$$\%S = 100 \times \frac{k}{N} \quad (4)$$

and thus $k = N \times (\%S/100)$. Adding the two broadening terms we obtain:

$$\beta_{\Delta 2\theta} \approx \frac{D}{N} + \frac{\%S}{100} \times \Delta_{ik} = \frac{D}{N} + \frac{k}{N} \times \Delta_{ik} = \frac{D}{N} + \frac{\delta_{ik}}{N} = \frac{C_{ik}}{N} \quad (5)$$

where %S is the percentage of expandable interlayers and D, k and $\beta_{\Delta\theta}$ have already been defined. The product $\delta_{ik} = k \times \Delta_{ik}$ is a broadening coefficient, for an 'i' swelling layer type and a given coefficient of proportionality k, which can be evaluated empirically. Then for a given k and a known Δ_{ik} or for known values of $\beta_{\Delta 2\theta}$ and N or $\beta_{\Delta 2\theta}$ and %S, the C_{ik} are determined. The index k denotes that Δ_{ik}, when deduced empirically, needs to be evaluated for each k value and swelling layer state 'i'.

Some justification for our use of eqn. (4) may be found by considering the Méring equation (Méring, 1949), which consists of two terms: (1) the Hendricks & Teller (1942) equation; and (2) the correction for finite crystallite size.

These two terms have a similar intensity ratio if an inverse relation is chosen between the number of layers and the number of expandable layers. In Fig. 4 we chose $k = 1$, but it can have a non-integer value. Surprisingly, for a given k (%S proportional to $1/N$) the SW of the Méring interference function is also consistent with a linear shape in an X-Y chart of SW *vs.* the inverse of N (Fig. 3 curve 6). It must be kept in mind that the proposed eqn. (5) is valid for large values of N (e.g. 30). For the IC method this limit indicates that eqn. (5) is valid from mid-anchizone (Jaboyedoff *et al.*, in prep.) to higher metamorphic conditions. By adding the variable k, two values are necessary to determine N, k and %S. This can be achieved by measuring two different SW.

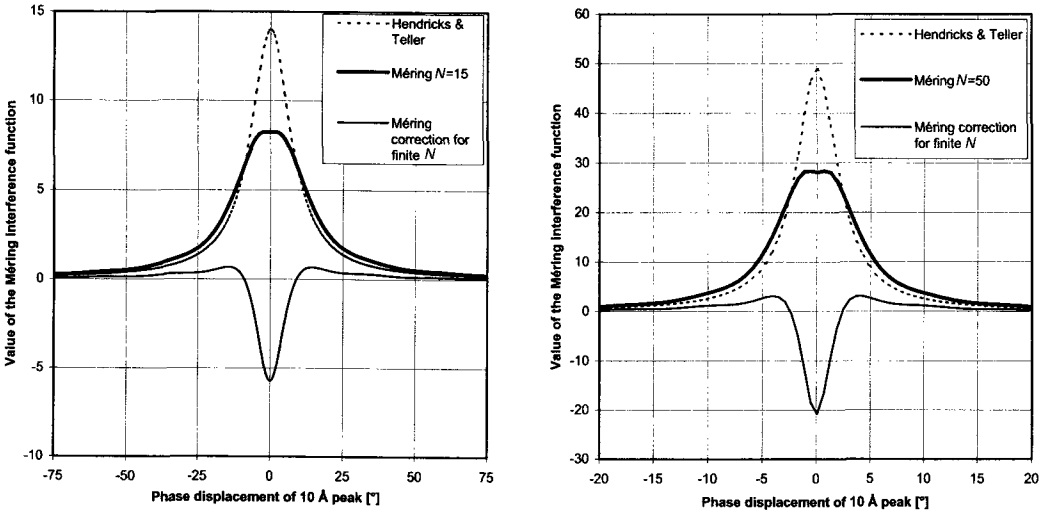

FIG. 4. The Méring interference function for different N, but calculated with the same k =1, displays the same behaviour. The Hendricks & Teller (1941) interference function, and the correction factor of the Méring equation are also shown.

C_{ik} AND Δ_{ik} DETERMINATION

Method 1 and the meaning of Δ_{ik}

For eqn. (5) an empirical meaning of the term Δ_{ik} can be given, leading to Method 1. For our purpose, it is sufficient to work in 2θ space. The principle of Méring (1949) (Moore & Reynolds, 1989) states that some peaks of a mixed-layer mineral lie between the peaks of the pure components. These positions are functions of the amount of mixed-layering. The peak position can be linearly dependent on the amount of the expandable component, but for small numbers of swelling layers and large CSD size, the peak maximum is not shifted because of the predominance of the major component. Considering a Markovian CSD distribution of the mixed-layer stacking, only the richest sequences (i.e. those CSDs with a relatively large number of swelling interlayers) possess shifted diffraction peaks, but their intensities are weaker than those with no expandable layers. As a result, in the case of weak mixed-layering, the mixed-layer diffraction peaks are only broadened and not shifted. Consequently, the broadening can be assumed to be equal or proportional to the mean displacement of the peak position of the mixed-layer mineral, equal to the expected peak position of the mixed-layer. Then, Δ_{ik} in eqn. (5) can be chosen as the absolute value of the difference in angle 2θ between the successive XRD peaks interfering from the two components, the swelling interlayer being of type '*i*'. For example, in the case of an air-dried sample of a mica-smectite interstratification, Δ_{ik} for the 10 Å peak may be taken as the difference in °2θ values of the 10 Å and 15 Å reflections (see Table 1). The k index can be cancelled, because Δ_i is identical for all k. For instance, if N is high, then the maximum intensity of the I-S mixed-layer minerals' diffraction peak will be that of the pure illite (mica-like layer), the expandable component producing only a broadening.

It must be pointed out that the linearity of the movement of the peak position is correct only if the *d*-spacings of the components are similar (Méring, 1949). In our case, this condition is not fully satisfied, but it is not very important, because we are dealing only with the broadening of the peak.

When using Δ_i (method 1) only one peak of each component of the mixed-layer mineral must interact. However, it is possible to use this method even if this condition is not verified. For example, in the case of I-S disordered interstratification (R0) of 10 Å and 15 Å thick layers, the Méring interference function is broadened by two smectite diffraction peaks. Actually the 001 peak of the pure illite (or dioctahedral mica) lies between the 001 and 002 peaks of an AD smectite (two water layers). Then broadening appears on both sides of the peak (Fig. 4), but the effects of the structure factor and the Lorentz-polarization factor tend to cancel the high-angle part of the broadening and enlarge the low-angle component (Fig. 5). Because of these two opposite effects, the SW of the Méring interference function is very similar whether or not the structure factor and the Lorentz-polarization factor multiply it (Fig. 3, curves 6, 7 and 8). This is also why the results obtained for the weighted Scherrer equation and Newmod© simulation are so similar. In addition it must pointed out that for a Reichweite R0, the SW of the Méring interference function is similar to the SW of the R0 Newmod© simulation of I-S with low %S (Fig. 3).

TABLE 1. C_{ik} estimations. To give an approximate value of C_{ik}, Δ_k can be taken to be the difference in °Δ2θ Cu-$K\alpha$ between the peak positions for the pure components; the numbers in parentheses give the percentage deviation of such values of C_{ik} from those obtained by Newmod© estimation.

$\%S = 100 \times \frac{k}{N}$	Two water (Newmod)	Two glycol (Newmod)	10–15 Å Estimation	10–8.5 (17) Å Estimation
Pure illite	7.68	7.68	7.89 (3%)	7.89
$k = 0.5$	9.20	8.64	9.36 (2%)	8.67 (<1%)
$k = 1$	11.04	9.68	10.84 (2%)	9.45 (3%)
$k = 2$	15.92	12.32	13.79 (14%)	11.02 (11%)
$k = 3$	22.00	15.52	16.74 (24%)	12.59 (19%)

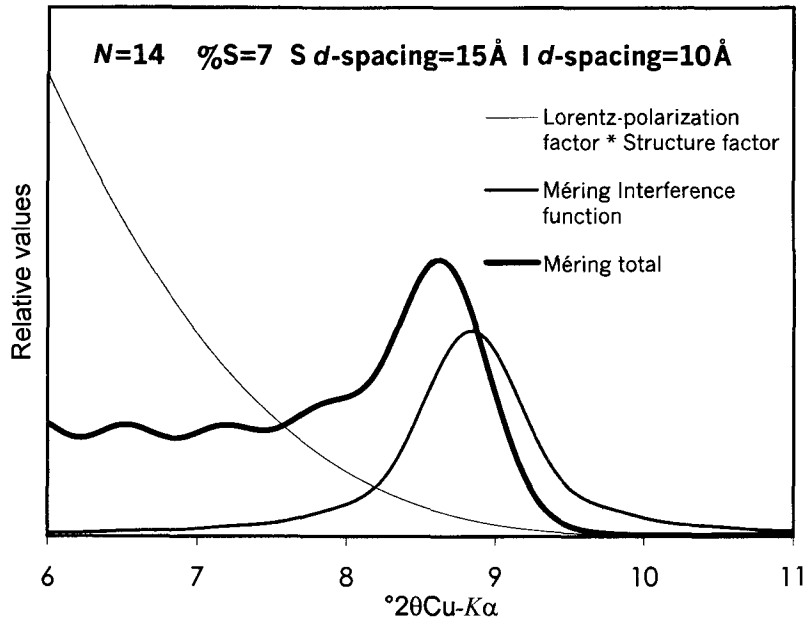

FIG. 5. Schematic view of the asymmetric effect caused by the structure factor (here dimica) and Lorentz-polarization factor on the Méring interference function giving the simulated spectrum (Méring Total). Note the steeper high-angle part and gentle low-angle part of the total simulation compared to the interference function. Modified after Moore & Reynolds (1997) for the Méring model. This remark is also valid for comparison between pure mica Newmod© simulation and weighted Scherrer equation (see Fig. 3).

Taking into account all those remarks, it is clear that the better solution is to deduce C_{ik} empirically by simulation. Nevertheless the order of magnitude is correctly deduced by the previous simple arguments (Table 1), when the goal is to perform simulations to compare it with the raw data.

To obtain values for N and %S the SW of the equivalent XRD peak on patterns from two differently treated specimens need to be measured. Putting $i = A$ and B and using eqn. (5), Δ_A and Δ_B being defined, k is given by:

$$k = \mathrm{D} \times \frac{(\mathrm{SW}_A - \mathrm{SW}_B)}{(\Delta_A \times \mathrm{SW}_B - \Delta_B \times \mathrm{SW}_A)} \qquad (6)$$

where SW_A and SW_B are the SW measured on the different XRD patterns, corrected for instrumental broadening effect, and D is defined in eqn. (3). The CSD size N is then given by:

$$N = \frac{\mathrm{D} + \Delta_i \times k}{\mathrm{SW}_i} \qquad (7)$$

where i is equal either to A or B.

Method 2: empirical determination of C_{ik}

In a SW–(1/N) graph, the relationships obtained using the different procedures, such as Newmod© simulations and interference functions are nearly linear (Figs. 3 and 6) for small SW corresponding to $N > \sim 30$ ($1/N = 0.033$). As already mentioned, it is better to evaluate C_{ik} by SW measurement on simulated XRD patterns of high CDS size, instead of using method 1, by:

$$C_{ik} = N_{\text{simulated}} \times \beta^{\text{simulated}}_{\Delta 2\theta, ik} \qquad (8)$$

where $\beta^{\text{simulated}}_{\Delta 2\theta, ik}$ is the SW of the chosen peak for a given treatment 'i' and a given k. In the following example we chose a mean value of $N = 80$ (range 70–90) to calculate the C_{ik}. Then the ratio $m_{A\text{-}B,k}$ of the corresponding SW measurements for a given k on two different treatments is a constant given by:

$$\frac{\mathrm{SW}_{Ak}}{\mathrm{SW}_{Bk}} = \frac{C_{Ak}}{C_{Bk}} = m_{A-B,k} \qquad (9)$$

Then if some $m_{A\text{-}B,k}$ are defined for various k, it is possible by a simple calculation to obtain k for

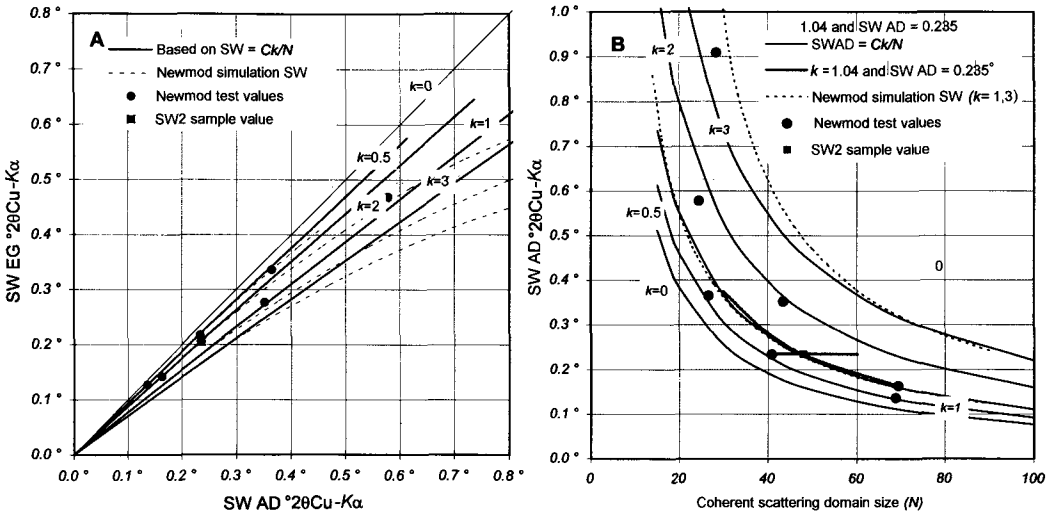

FIG. 6. (A) Example of a SWAD-SWEG chart presenting results from Newmod© simulation for R0 (dashed lines) and linear results obtained with an estimation of C_k based on a couple of simulations with $N = 70-90$ for $k = 0.5, 1, 2, 3$. The approximation is valid up to SW (AD) of 0.40°Δ2θ Cu-$K\alpha$. (B) N-SWAD for two water layers used to determine N compared with two curves obtained by simulation. The points are from Tables 3 and 4 and Fig. 7. The interpolation for the k curve can be observed for sample SW2. The instrumental broadening (fifth effect) must be removed to use these charts.

the SW measured on XRD patterns of the same sample treated by two different methods. On the basis that $m_{A\text{-}B,x}$ is the ratio of two SW, the index 'x' indicates that k is unknown for the sample. From the defined $m_{A\text{-}B,k}$ (eqn. 9), the two nearest $m_{A\text{-}B,k1}$ and $m_{A\text{-}B,k2}$ of known k, which are smaller and greater than $m_{A\text{-}B,x}$ respectively, can be found. It is clear from eqn. (5) that $k_1 < k_2$. Then k can be evaluated by using:

$$k = k_1 + (k_2 - k_1)\frac{m_{A-B,k_x} - m_{A-B,k_1}}{m_{A-B,k_2} - m_{A-B,k_1}} \qquad (10)$$

In order to understand the previous approach better, it is possible to create SWAD-SWEG charts by plotting the curves for given constant k (Fig. 6). Plotting data points on such a diagram allows us to determine k, by comparison with the k-isolines obtained by calculations. Values for N can be determined on other charts linking SW to CSD size for the known k, like N-SWAD or N-SWEG charts (Fig. 6B). The trajectory of the estimated k is then evaluated, N determined, and %S is calculated by relation (3).

Those charts can also be established for different Reichweite (Fig. 3). For Reichweite R1, this approximation is valid up to SW $\approx$ 0.40°Δ2θ Cu-$K\alpha$ and for slightly smaller SW for R3. The validity of this new equation decreases with increasing k (Fig. 3; Jaboyedoff *et al.*, in prep.).

RESULTS

In order to check the validity of the methods, we tested them on simulations and compared the results obtained from a natural sample by Newmod© simulation. The following parameters were used in the Newmod© simulations: d-spacing of dioctahedral mica = 9.98 Å, dioctahedral smectite-2 glycol layers = 16.9 Å; dioctahedral smectite-2 water layers = 15 Å; Ca exchange cation; 0.9 K and 0.1 Fe per $(Si,Al)_4O_{10}$ for dioctahedral mica and 0.1 Fe per $(Si,Al)_4O_{10}$ for dioctahedral smectite; 0.5° divergent slit; Cu-$K\alpha$ radiation; 18.5 cm goniometer radius, sample length 2.8 cm and two Soller slits of 5°.

For I-S with low expandable layer content, it is possible to obtain two or more SW values (from XRD patterns of AD, EG, and heated at 300°C for 12 h, preparations) to determine k. The swelling interlayers of the AD pattern are supposed to contain two water layers (2W), the EG pattern, two ethylene glycol (2G) layers and the heated sample, no interlayer. In order to have information on peaks

TABLE 2. Comparison between the results of method 1 and the Scherrer equation obtained for the Méring interference function. Abbreviations are used as in the text. Dev means deviation from the true values. 2W are the results for the Scherrer equation on AD preparation and 2G for EG preparation (for Newmod© simulations no instrumental broadening effect is present, except the Lorentz factor).

Data						Estimations							
Méring interference function						Method 1					Scherrer		
Peak	Mean N	%S	k	SW AD	SW EG	N	Dev	%S	Dev	k	2W	2G	%S
10 Å	20	3.0%	0.60	0.49°	0.45°	20	0	3.0%	0.0%	0.59	16	18	0%
5 Å	20	3.0%	0.60	0.39°	0.48°	20	0	4.4%	1.4%	0.89	20	17	0%
10 Å	45	2.0%	0.90	0.24°	0.22°	43	−2	1.9%	−0.1%	0.81	33	37	0%
5 Å	45	2.0%	0.90	0.17°	0.23°	46	1	2.8%	0.8%	1.30	46	34	0%
10 Å	70	1.5%	1.05	0.16°	0.14°	66	−4	1.4%	−0.1%	0.95	49	55	0%
5 Å	70	1.5%	1.05	0.11°	0.16°	71	1	2.1%	0.6%	1.52	71	51	0%
10 Å	20	6.0%	1.20	0.63°	0.52°	20	0	8.0%	2.0%	1.61	12	15	0%
5 Å	20	6.0%	1.20	0.39°	0.59°	21	1	10.0%	4.0%	0.84	21	14	0%

unaffected by instrumental effects or by those of the structure factor, we tested method 1 on Méring 9.98 Å and 4.99 Å peaks. It can be seen in Table 2 that results are in good agreement with the data, especially for the ~10 Å peak, in spite of the double interference of the two smectite peaks for the AD pattern. The results become less accurate for $N = 20$ due to the limitations of the method, especially when %S>5%, but for such values of N and %S the peak position method begins to be applicable. From eqn. 7 it can be seen that the results for the ~5 Å peak give N equal to the Scherrer equation when used for AD preparation, since $\Delta_i = 0$ for this peak. Compared to the N mean value, used for the simulation, the 5 Å peak results are almost exact.

Method 1 was used to determine N and %S directly on Newmod© simulations (Tables 3 and 4), and the results are in good agreement with the simulated data. The ~10 Å peak results for %S are better than those of the ~5 Å. The explanation for the slightly higher N value of the 5 Å peak, cannot be ascribed to the rms problem, because the difference between the standard mean and the rms is no more than 0.2 layer. It can be seen again that the method becomes inaccurate when N is <25 and %S >5%, where the peak position method becomes efficient. The 10 Å peak gives no reasonable solution for %S = 9.2.

Method 2 applied to the ~10 Å peak yields more consistent results than the other method. The N estimations are equivalent to the method 1, but %S is more accurate (Tables 3 and 4). Only the 9.2 %S is significantly different.

In order to demonstrate the efficiency of such methods, XRD patterns of a natural sample were compared to XRD patterns generated by Newmod© simulations according to method 2. The sample SW2 comes from the CIS standards, used for the ISW method (10 Å peak), described in Warr & Rice (1994). Its metamorphic grade corresponds to the diagenesis-anchizone limit. The measured ISW on our diffractometer are 0.32° and 0.29°Δ2θ Cu-$K\alpha$ for the AD and EG specimens, respectively. Corrected for instrumental broadening by the method outlined above, those values are 0.24° and 0.21°Δ2θ Cu-$K\alpha$ leading to $N = 48$, %S = 2.2% and $k = 1.04$ (method 1 gives very similar results $N = 47$, %S = 2.3% and $k = 1.06$). We performed simulations for AD (two water layers) EG (two glycol layers) and heated for 12 h at 300°C (pure mica) preparations with N = 38–58, %S = 2.2% and a d-spacing of the illite of 10.06 Å (other parameters are the same as listed above). In order to compare the raw data with the Newmod© simulations of the ~10 Å peak, the simulations have been convoluted with the instrumental profile (a mica powder peak) and multiplied by a coefficient and a constant was added to simulate the observed background (Fig. 7). It is clear that the order of magnitude of the mean CSD size and the mean %S are correct; the small difference can be attributed to two different sources: (1) the CSD size distribution of the sample is certainly spread out over a broader range with an asymmetric log-normal distribution rather than that used in the simulations; and (2) the sample contains a mixture of a detrital mica with

TABLE 3. Comparison between the results of methods 1 and 2 and the Scherrer equation obtained on normal Newmod simulations for the 10 Å I-S peak. Abbreviations are used as in Table 2. Ranges of N values with equal probability are indicated.

Data						Estimations											
Newmod 10 Å simulations						Method 1					Scherrer			Method 2				
N range	Mean N	%S	k	SW AD	SW EG	N	Dev	%S	Dev	k	2W	2G	%S	N	Dev	%S	Dev	k
20 to 30	25	2.4%	0.60	0.37°	0.34°	26	1	2.2%	−0.2%	0.57	22	23	0%	27	2	2.4%	0.0%	0.65
35 to 45	40	1.5%	0.60	0.23°	0.22°	40	0	1.3%	−0.2%	0.52	34	36	0%	41	1	1.5%	0.0%	0.59
65 to 75	70	0.9%	0.60	0.14°	0.13°	68	−2	0.7%	−0.2%	0.46	58	62	0%	69	−1	0.8%	−0.1%	0.54
15 to 25	20	5.5%	1.10	0.58°	0.47°	24	4	8.2%	2.7%	1.9	14	17	0%	24	4	6.7%	1.2%	1.64
65 to 75	70	1.6%	1.10	0.16°	0.14°	68	−2	1.6%	0.0%	1.1	48	56	0%	69	−1	1.52%	0.0%	1.05
35 to 45	40	4.0%	1.60	0.35°	0.28°	42	2	5.7%	1.7%	2.4	22	29	0%	43	3	4.31%	0.3%	1.87
20 to 30	25	9.2%	2.30	0.91°	0.51°	–	–	–	–	–	–	–	–	28	3	17.7%	8.5%	5.05

TABLE 4. Comparison between the results of method 1 and the Scherrer equation obtained on normal Newmod simulations for the 5 Å peak as Table 3. The 2W Scherrer equation estimations are equal to the N estimations.

Data						Estimations							
Newmod 5 Å simulations						Method 1					Scherrer		
N range	Mean N	%S	k	SW AD	SW EG	N	Dev	%S	Dev	k	2W	2G	%S
20 to 30	25	2.4%	0.60	0.29°	0.37°	27	2	3.5%	1.1%	0.96	25	22	0%
35 to 45	40	1.5%	0.60	0.19°	0.23°	42	2	2.1%	0.6%	0.87	40	34	0%
65 to 75	70	0.9%	0.60	0.11°	0.13°	72	2	1.2%	0.3%	0.82	70	59	0%
15 to 25	20	5.5%	1.10	0.36°	0.54°	22	2	9.4%	3.9%	2.1	20	15	0%
65 to 75	70	1.6%	1.10	0.11°	0.16°	72	2	2.3%	0.7%	1.6	70	51	0%
35 to 45	40	4.0%	1.60	0.19°	0.33°	42	2	6.8%	2.8%	2.9	40	24	0%
20 to 30	25	9.2%	2.30	0.29°	0.67°	28	3	19.3%	10.1%	5.3	25	12	0%

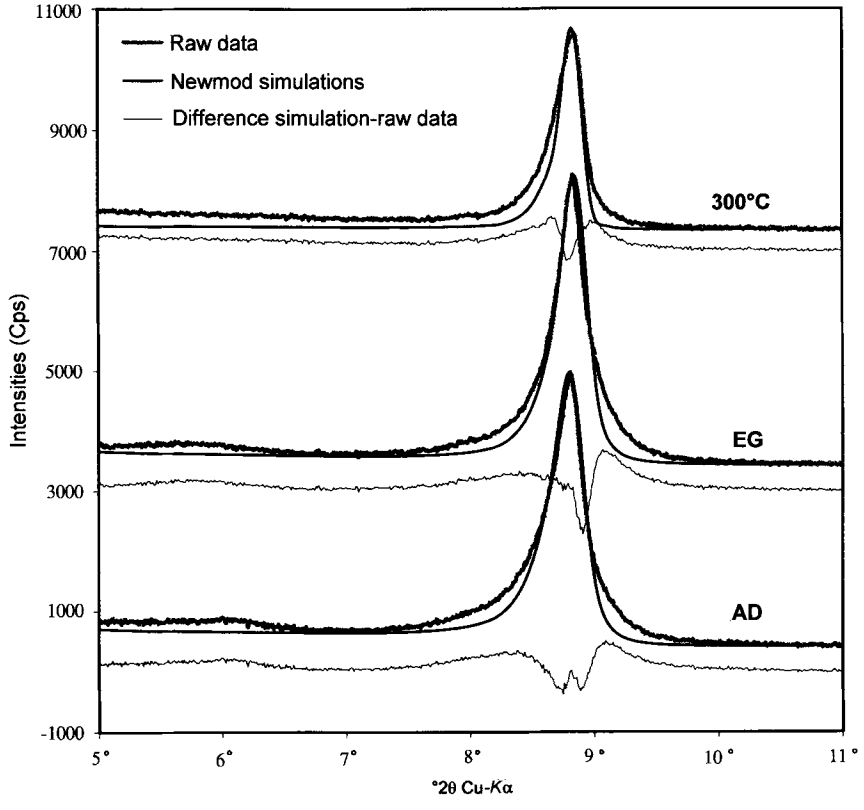

FIG. 7. Comparison between raw data and simulations. The Newmod simulations are based on $N = 38-58$, %S = 2.2% determined from method 2. The purely numerical method gives $N = 47$ and %S = 2.3, the mica d-spacing has been changed to 10.06 Å because of the sample. The heated pattern was moved by $0.06°\Delta 2\theta$ Cu-$K\alpha$ because some defocalization occurs. For the EG the Newmod simulation was multiplied by 0.61 and a linear background of 420 cps added. For the AD pattern those numbers are 0.63 and 420 respectively, and for the heated example 0.30 and 350, respectively. The XRD patterns are shifted slightly with respect to the quartz peak position, also caused by the convolution. (Data were collected on a Rigaku Geigerflex diffractometer on oriented sedimented slide: sample length = 28 mm, Goniometer radius = 185 mm, radiation Cu-$K\alpha$ filter Ni-$K\beta$, current 40 kV/30 mA, Proportional counter, receiving slit = 0.047°, divergent slit = 0.5°, soller slits = 5°–5°, step scan, step 0.01°, 2 s/step).

large N and a mixed-layer I-S with smaller N than that deduced by the present method.

Those two solutions will keep the mean CSD size constant but vary the CSD size variance; the explanation of the error on %S is more complicated. Starting from these results, it will be easier to adjust the model to give a more realistic solution than starting with no information for N and %S.

Our results are not in accordance with those from the CIS scale ($N = 18.5$ and %S = 0). This may indicate a problem with the manner in which we have performed the CIS calibration and we are currently trying to find the source of this problem. Nevertheless, using our calibration with the CIS scale the IC (SWAD value) leads to $N = 17$, compatible with the standard value. Because our purpose is to demonstrate the efficiency of both methods, the calculations were performed for Rechweite R0, but the Reichweite of the sample is probably higher and in this case, method 2 has to be applied, which will probably lead to lower values.

Method 1 is also applicable to other mixed-layer minerals. Here we checked the result obtained for

tri-trioctahedral chlorite weakly interstratified with trioctahedral smectite (C-S). This case is interesting because the results are more consistent if values of Δ_i are 'calibrated' by using preliminary simulation. A good example is the use of the 7.1 Å diffraction peak of C-S (see Table 5). The Scherrer equation used for the peak of the AD (two water layers) simulation is consistent with the exact values for the CSD size; this is also valid in the case of the Méring interference function alone. Then the Δ_i used in method 1 for AD (Δ_{2w}) calculation can be set to zero in order to obtain the correct N and the Δ_i used for the EG parameter can be set to the peak position difference 002 chlorite - 002 smectite-2EG layers. We have checked that the results are better than if we use the peak difference for Δ_{2w}. The results are relevant, but as already mentioned, with N <20 and/or %S>5%, the method begins to fail. The same applies to the 14.2 Å (Table 6) and the 7.1 Å peaks, when method 1 is applied with the standard definitions of Δ_i. However, in this case the structure factor and the Lorentz polarization factor are more influential, and therefore the determination of N is less accurate than the Scherrer equation but the %S is more reliable.

DISCUSSION AND CONCLUSIONS

When the relation between %S is chosen as inversely proportional to N, i.e. fixed by a %S = k/N relation, it seems clear that the SW of the Méring interference function and Newmod© simulations present linear relations between SW and the inverse of N for small SW (Fig. 3). Because an additional variable k is added, two SW values are needed to determine k and N or k and %S, instead of one for the Scherrer equation. The parameters, C_{ik} and Δ_{ik}, needed to perform the proposed methods can either be computed with the help of Newmod© simulations or estimated by simple computation of judiciously chosen XRD peak position differences between the two mixed-layer components. The use of simulations to obtain some C_{ik} values directly gives more accurate results. For example, the charts created with a few Newmod© simulations are consistent with charts constructed with several XRD pattern simulations, but only for small SW (Fig. 6). This is also true for a Reichweite R1 as demonstrated in Fig. 3, but in this case only method 2 is applicable.

Because of the difficulties in obtaining information on mixed-layer minerals with N>100 when SWAD>SWEG, the formula presented here is a unique tool to determine an order of magnitude estimate of the percentage of expandable interlayers and the mean value of N. For N>100 the result will be very sensitive to the procedure used to remove instrumental effects, but when SW are different for different treatments, it is interesting to have an estimate of the number of swelling layers. We used this method in a computer program based on several Newmod© I-S simulations, which will soon be available on the web (Jaboyedoff *et al.*, in prep). Furthermore, the approximations assumed in this study are better when N is high. However, the results obtained even for N<30 are correct to an acceptable order of magnitude, provided %S is not greater than 5%; above this value the peak maximum begins to shift and then the expandable layer effect is not ascribable simply to peak broadening. However, in such cases the peak position method begins to be accurate. When the d-spacing of the two reflections from the end-members of the interstratification are identical, the Scherrer equation can be used directly to estimate the CSD size. This has already been discussed by Nieto & Navas-Sanchez (1994), Arkai *et al.* (1996) and Warr (1996) for the 5 Å diffraction peak for I-S.

The empirical calculation of C_{ik}, by estimation of Δ_i from peak positions leads to reasonable values (Tables 1–6). This method is then useful to rapidly estimate N and the content of swelling layers for other mixed-layer minerals. The method is therefore a good tool to obtain preliminary information to simulate an XRD pattern in order to quantify the parameters. In the case of I-S interstratification, heated or other saturated sample preparations can be an aid in the determination of either N and %S or to reveal the nature of other effects, such as the presence of more than two components in the mixed-layering. A common cause of such an effect is the problem of the hydration of the expandable interlayers. Sometimes only one water layer remains in some interlayers, thus leading to a three-component mixed-layering (Jaboyedoff & Thélin, 1996). In this case, SWAD < SWEG may be observed, being the result of expandable layers containing less than two water layers, (Jaboyedoff *et al.*, in prep.).

Few methods exist for quick estimates of mixed-layer minerals containing small amounts of swelling interlayer. This indicates that such a method can certainly be applied to types of mixed-layer minerals other than I-S and C-S.

TABLE 5. Comparison between the results of method 1 and the Scherrer equation obtained on normal Newmod simulations for the C-S 7 Å peak. Abbreviations are as used in Table 2. The range of N values with equal probability are indicated, or single N (70) or with free defects distance (35). The chemical composition used in the Newmod simulations is 1 Fe per $(Si,R^{3+})_4O_{10}$ in the 2:1 layer and 1 Fe in the interlayer octahedral sheet $(R^{2+})_3OH_6$.

			Data			Estimations							
			Newmod 7.1 Å simulations			Method 1					Scherrer		
N range	Mean N	%S	k	SW AD	SW EG	N	Dev	%S	Dev	k	2W	2G	%S
15 to 35	25	2.5%	0.63	0.21°	0.26°	26	1	2.3%	−0.2%	0.60	26	21	0%
40 to 60	50	1.5%	0.75	0.11°	0.14°	49	−1	1.3%	−0.3%	0.61	49	40	0%
20 to 40	30	3.0%	0.90	0.19°	0.24°	30	0	2.8%	−0.2%	0.84	30	23	0%
70	70	2.0%	1.40	0.09°	0.12°	66	−4	1.8%	−0.2%	1.18	66	46	0%
2 to 70	35	5.0%	1.75	0.14°	0.27°	41	6	6.9%	1.9%	2.82	41	20	0%
10 to 30	20	13.0%	2.60	0.28°	0.64°	20	0	18.7%	5.7%	3.61	20	9	0%

TABLE 6. As for Table 5 but for the 14.2 Å peak.

			Data			Estimations							
			Newmod 14.2 Å simulations			Method 1					Scherrer		
N range	Mean N	%S	k	SW AD	SW EG	N	Dev	%S	Dev	k	2W	2G	%S
15 to 35	25	2.5%	0.63	0.18°	0.19°	32	7	2.0%	−0.5%	0.63	31	29	0%
40 to 60	50	1.5%	0.75	0.10°	0.11°	58	8	1.2%	−0.3%	0.70	55	51	0%
20 to 40	30	3.0%	0.90	0.16°	0.17°	38	8	2.4%	−0.6%	0.91	36	32	0%
70	70	2.0%	1.40	0.08°	0.09°	78	8	1.5%	−0.5%	1.17	73	64	0%
2 to 70	35	5.0%	1.75	0.12°	0.16°	56	21	6.5%	1.5%	3.65	46	34	0%
10 to 30	20	13.0%	2.60	0.23°	0.31°	30	10	12.7%	−0.3%	3.80	24	18	0%

ACKNOWLEDGMENTS

Financial support for this work was provided by the Swiss National Science Foundation, projects number 21-26433.89 and 20-31234.91 and by the Dourakine Institute. The Institute of Mineralogy of Lausanne University and the Institute of Geology of Neuchâtel University kindly provided the logistical support. T. Adatte, C. Bauchau, F. Bussy, A.-C. Gerber, F. Girod and D. Kirschner are thanked for their suggestions which improved the manuscript. The encouragement of J.L. Epard, A. Escher and M. Sartori was greatly appreciated. L.N. Warr and an anonymous reviewer made helpful, constructive remarks on the structure, content and English syntax of the manuscript, and are warmly thanked.

REFERENCES

Arkai P., Balogh K. & Frey M. (1997) The effects of tectonic strain on crystallinity, apparent mean crystallite size and lattice strain of phyllosilicates in low-temperature metamorphic rocks. A case study from the Glarus overthrust, Switzerland. *Schweiz. Mineral. Petrogr. Mitt.* **77**, 27–40.

Arkai P., Merriman R.J., Roberts B., Peacor D.R. & Toth M. (1996) Crystallinity, crystallite size and lattice strain of illite-muscovite and chlorite: comparison of XRD and TEM data for diagenetic to epizonal pelites. *Eur. J. Mineral.* **8**, 1119–1137.

Balasingh C., Abuhasan A., & Predecki P.K. (1991) Diffraction peak broadening studies in Al_2O_3 (wishker) composites. *Powder Diffr.* **6**, 16–19.

Delhez R., de Keijser T.H. & Mittemeijer E.J. (1982) Determination of crystallite and lattice distortions through X-ray line profile analysis. Recipes, methods and comments. *Fresenius Z. Anal. Chem.* **312**, 1–16.

Drits V.A. & Tchoubar C. (1990) *X-ray Diffraction by Disordered Lamellar Structures*. Springer Verlag, Berlin.

Drits V.A., Eberl D.D. & Środoń J. (1997) XRD measurement of mean crystallite thickness of illite and illite/smectite: reappraisal of the Kübler Index and the Scherrer Equation. *Clays Clay Miner.* **45**, 461–475.

Drits V.A., Eberl D.D. & Środoń J. (1998) XRD measurement of mean thickeness, thickness distribution and strain for illite and illite-smectite crystallites by Bertaut-Warren-Averbach technique. *Clays Clay Miner.* **46**, 38–50.

Eberl D.D., & Blum A. (1993) Illite crystallite thickness by X-ray diffraction. Pp. 124–153 in: *Computer Applications to X-ray Powder Diffraction Analysis of Clay Minerals* (R.C. Reynolds & J.R. Walker, editors). Clay Minerals Society, Special Publication **5**, Bloomington, Indiana.

Eberl D.D. & Velde B. (1989) Beyond the Kübler index. *Clay Miner.* **24**, 571–577.

Eberl D.D., Drits V.A. & Środoń J. (1997) Measurement of illite crystallite thickness by XRD method of Bertaut-Warren-Averbach. Pp. 27–28 in: Journée Scientifiques en l'honneur de V.A. Drits, *Groupe Française Argiles*. Paris.

Eberl D.D., Nuesch R., Šucha V. & Tsipurski S. (1998) Measurement of fundamental illite particle thicknesses by XRD using PVP-10 intercalation method of Bertaut-Warren-Averbach. *Clays Clay Miner.* **46**, 89–97.

Ergun S. (1968) Direct method for unfolding convolution products – its application to X-ray scattering intensities. *J. Appl. Cryst.* **1**, 19–23.

Frey M. (1987) *Low Temperature Metamorphism*. Chapman & Hall, London.

Frey M. (1988) Discontinuous inverse metamorphic zonation, Glarus Alps, Switzerland: evidence from illite "crystallinity" data. *Schweitz. Mineral. Perogr. Mitt.* **68**, 171–183.

Goy-Eggenberger D. & Kübler B. (1990) Résultats préliminaires d'un essai de zonéographie métamorphique à travers les formations calcaires de la Nappe de Morcles. *Schweiz. Mineral. Petrogr. Mitt.* **70**, 83–88.

Hendricks S.B. & Teller E. (1941) X-ray interference in partially ordered layer lattices. *J. Phys. Chem.* **10**, 147–167.

Jaboyedoff M. (1999) *Transformations des interstratifiés illite/smectite vers l'illite et la phengite: un exemple dans la série carbonatée du domaine Briançonnais des Alpes suisses romandes*. PhD thesis, Univ. Lausanne, Switzerland.

Jaboyedoff M. & Thélin P. (1996) New data on low metamorphism in the Briançonnais domain of Prealps, Western Switzerland. *Eur. J. Mineral.* **8**, 577–592.

Jaboyedoff M., Kübler B. & Thélin P. (in prep.) Illite crystallinity revisited. *Clays Clay Miner.*

Jagodzinski H. (1949) Eindimensionale Fehlordnung in Kristallen und ihr Einfluss auf Röntgeninterferenzen. I. Berechnung des Fehlordnungsgrades aus des Röntgenintensitäten. *Acta Crystallogr.* **2**, 201–207.

Klug H.P. & Alexander L.E. (1974) *X-ray Diffraction Procedures*. J. Wiley & Sons, New York.

Kodama H., Gatineau L. & Méring J. (1971) An analysis of X-ray diffraction line profiles of microcrystalline muscovites. *Clays Clay Miner.* **19**, 405–413.

Krumm S. (1992) Methodishe Untersuchungen, regionale Anwendungen und Verlgleiche mit anderen Parametern. *Erlanger geol. Abh.* **120**, 1–75.

Kübler B. (1964) Les argiles, indicateurs de métamorphisme. *Rev. Inst. Franç. Pétrol.* **XIX**, 1093–1112.

Kübler B. (1967) La cristallinité de l'illite et les zones tout à fait supérieures du métamorphisme. Pp. 105–121 in: *Etages tectoniques, Colloque de Neuchâtel 1966*. (de la Baconnière, editor).

Neuchâtel, Switzerland.

Kübler B. (1968) Evaluation quantitative du metamorphisme par cristallinité de l'illite. *Bull. Centre Rech. Pau SNPA* **2**, 385–397.

Kübler B. (1984) Les indicateurs des transformations physiques et chimiques dans la diagenèse, température et calorimétrie. Pp. 489–596 in: *Thermométrie et barométrie géologiques* (M. Lagache, editor). Soc. Franç. Miner. Crist., Paris.

Kübler B. (1990) "Cristallinité" de l'illite et mixed-layer: brève révision. *Schweiz. Mineral. Petrogr. Mitt.* **70**, 89–93.

Langford J.I. & Wilson J.C. (1978) Scherrer after sixty years: a survey and some new results in the determination of crystallite size. *J. Appl. Cryst.* **11**, 102–113.

Lanson B. (1990) *Mise en évidence des mécanismes de transformation des interstratifiés illite/smectite au cours de la diagenèse.* PhD thesis, Univ. Paris 6, France.

Lanson B. & Champion D. (1991) The I/S-to-illite reaction in the late stage diagenesis. *Am. J. Sci.* **291**, 473–506.

Lanson B. & Velde B. (1992) Decomposition of X-ray diffraction patterns: a convenient way to describe complex I/S diagenetic evolution. *Clays Clay Miner.* **40**, 629–643.

Méring J. (1949) L'interférence des rayons X dans les systèmes à interstratification désordonnée. *Acta Cryst.* **2**, 371–377.

Merriman R.J., Roberts B. & Peacor D.R. (1990) A transmission electron microscope study of white mica crystallite size distribution in mudstone to slate transitional sequence, North Wales, UK. *Contrib. Mineral. Petrol.* **106**, 27–40.

Moore D.M. & Reynolds R.C. (1997) *X-ray Diffraction and the Identification and Analysis of Clay Minerals, 2nd edition.* Oxford University Press, Oxford and New York.

Nieto F. & Sanchez-Navas A. (1994) A comparative XRD and TEM study of the physical meaning of the white mica "crystallinity" index. *Eur. J. Mineral.* **6**, 611–621.

Pevear D.R. & Schuette S.F. (1993) Inverting the Newmod X-ray diffraction forward model for clay minerals using genetic algorithms. Pp. 123–153 in: *Computer Application to X-ray Powder Diffraction Analysis of Clay Minerals* (R.C. Reynolds & J.R. Walker, editors) Clay Minerals Society, Special Publication **5**, Bloomington, Indiana.

Reynolds R.C. (1968).The effect of particle size on apparent lattice spacings. *Acta Cryst.* **A24**, 319–320.

Reynolds R.C. (1980) Interstratified clay minerals. Pp. 249–303 in: *Crystal Structures of Clay Minerals and their X-ray Identification* (G.W. Brindley & G. Brown, editors). Monograph N°5. Mineralogical Society, London.

Reynolds R.C. (1985) NEWMOD a computer program for the calculation of one-dimensional diffraction patterns of mixed-layered clays. Published by the author, 8 Brook Dr., Hanover, New Hampshire, USA.

Reynolds R.C. (1989) Diffraction by small and disordered crystals. Pp. 145–182 in: *Modern Powder Diffraction* (D.L. Bisch & J.E. Post, editors). Reviews in Mineralogy **20**. Mineralogical Society of America, Washington D.C.

Reynolds R.C. & Reynolds R.C. (1996) *NEWMOD for Windows a computer program for the calculation of one-dimensional diffraction patterns of mixed-layered clays.* Published by the author, 8 Brook Dr., Hanover, New Hampshire, USA.

Roberts B. & Merriman R.J. (1985) The distinction between Caledonian burial and regional metamorphism in metapelites from North Wales: an analysis of isocryst patterns. *J. Geol. Soc.* **142**, 615–624.

Sassi R., Arkai P., Lantai C. & Venturini C. (1995) Location of boundary between the metamorphic Southalpine basement and the Paleozoic sequences of the Carnic Alps: illite "crystallinity" and vitrinite reflectance data. *Schweiz. Mineral. Petrogr. Mitt.* **75**, 399–412.

Scherrer P. (1918) Bestimmung der grosse und inneren Struktur von Kolloidteilchen mittels Röntgenstrahlen. *Nachr. Ges. Wiss. Göttingen*, **26**, 98–100.

Środoń J. & Eberl D.D. (1984) Illite. Pp. 495–544 in: *Micas.* (S.W. Bailey, editor) *Reviews in Mineralogy*, **13**. Mineralogical Society of America, Washington D.C.

Stern W.B., Mullis J. & Frey M. (1991) Deconvolution of the first "illite" basal reflection. *Schweiz. Mineral. Petrogr. Mitt.* **71**, 453–462.

Stokes A.R. (1948) A numerical Fourier-analysis method for correction of widths and shapes of lines on X-rays powder photographs. *Proc. Phys. Soc. London*, **61**, 382–391.

Wang H., Stern W.B. & Frey M. (1995) Deconvolution of the X-ray "Illite" 10 Å complex: a case study of Helvetic sediments from eastern Switzerland. *Schweiz. Mineral. Petrogr. Mitt.* **75**, 187–199.

Warr L.N. (1996) Standardized clay mineral crystallinity data from the very low-grade metamorphic facies rocks of southern New Zealand. *Eur. J. Mineral.* **8**, 115–127.

Warr L.N., & Rice H.N. (1994) Interlaboratory standardization and calibration of clay mineral crystallinity and crystallite size data. *J. metam. Geol.*, **12**, 141–152.

Warren B.E. & Averbach B.L. (1950) The effect of cold work distortion on X-ray patterns. *J. Appl. Phys.* **21**, 595–599.

Watanabe T. (1988) The structural model of illite/smectite interstratified minerals and the diagram for

its identification. *Clay Sci.* **7**, 97–114.

Weaver C.E. (1960) Possible uses of clay minerals in the search for oil. *Bull. Am. Assoc. Petrol. Geol.* **44**, 1505–1518.

Wilson A.J. (1962) On the variance as a measure of line broadening in diffractometry general theory and small particle size. *Proc. Phys. Soc. London*, **80**, 286–294.